

# Vertical Structures and Microphysical Mechanisms of Meiyu Precipitation Using Wind Profile Radar

<sup>1</sup>K. Krishna Reddy, <sup>2</sup>V. Adinarayana

<sup>1</sup>Professor, Department of Physics, Yogi Vemana University, Kadapa

<sup>2</sup>Lecturer, Department of Physics, Govt. College for Men(A), Kadapa

DOI: <https://doi.org/10.51244/IJRSI.2025.120500107>

Received: 22 May 2025; Accepted: 27 May 2025; Published: 13 June 2025

## ABSTRACT

This study investigates the vertical structure and temporal evolution of Meiyu precipitating cloud systems over Dongshan, China, utilizing data from an L-band Wind Profiler Radar (WPR) collected during the Intensive Observation Periods (IOPs) of 2001 and 2002. The WPR provides crucial insights into hydrometeor characteristics and vertical air motion by measuring reflectivity, reflectivity-weighted fall speed, and variance of hydrometeor fall speeds. Observations from June 2001 revealed the complex interaction between a Meiyu front and Typhoon Chebi (0102), illustrating how their movements influenced precipitation patterns. Detailed WPR data showed varied vertical rainfall structures, with horizontal mixing of rain mass in the lowest 2 km and a distinct bright band near 4.5 km indicating stratiform precipitation. Doppler vertical velocity measurements largely indicated stratiform structures with downward velocities, though weak updrafts were observed within the Meiyu frontal system. An X-band Doppler Radar comparison showed less precipitation in IOP-2001 compared to IOP-2002, with notable diurnal variations in the latter. A key aspect of this research involved classifying Meiyu precipitating clouds into convective, transition, and stratiform types using a WPR-based algorithm that assesses the presence of a melting layer and turbulence/hydrometeors. Convective regions exhibited strong updrafts and high reflectivity, while stratiform areas showed weaker vertical velocities and a clear bright band. Analysis of occurrence percentages revealed that IOP-2001 was dominated by mixed and stratiform clouds, whereas IOP-2002 had a more balanced distribution of convective and stratiform types. These differences were attributed to variations in atmospheric moisture content (relative humidity, precipitable water) and local environmental conditions (CAPE, CIN). This research highlights the effectiveness of WPR data in understanding Meiyu rainfall mechanisms and their potential for improving cloud-scale and mesoscale numerical models, ultimately aiding in better predictions and flood disaster mitigation efforts in East Asia.

## INTRODUCTION

The Meiyu season, also known as Changma in Korea and Baiu in Japan, typically occurs from mid-June to mid-July over the Yangtze-Huai River basin [1]. This rainy season is crucial for the water cycle in eastern China, contributing up to 50% of the annual precipitation [1]. The heavy rainfall often leads to floods, making accurate monitoring and prediction essential [2,3]. Recent studies, including those utilizing advanced modeling techniques, continue to emphasize the complexity and importance of accurately simulating Meiyu precipitation, especially in the context of extreme events [4].

The Meiyu front's activity is significantly influenced by the Asian monsoon and the North Pacific subtropical high. This quasi-stationary front, extending from western China to western Japan during summer, is crucial for longitudinal energy and moisture transport [5, 6]. It's characterized by a weak temperature gradient, strong vertical wind shear, and a large low-level moisture gradient.

Embedded precipitation systems within the Meiyu front are primarily convective. Numerous field experiments have been conducted to study these phenomena. The Taiwan Area Mesoscale Experiment (TAMEX) investigated heavy precipitation linked to low-level jets in Taiwan [7]. The South China Sea Monsoon Experiment (SCSMEX) aimed to understand summer monsoon onset and evolution in Southeast Asia and

southern China [8]. The Huaihe River Basin Experiment (HUBEX) focused on energy and hydrological processes of Meiyu frontal cloud systems and their land-surface interactions using Doppler radars, radiosondes, and surface meteorological stations [9]. The increasing frequency and intensity of extreme precipitation events during the Meiyu season underscore the ongoing need for detailed observational studies [10].

Given the limited opportunities to observe frequent Meiyu frontal heavy rainfall, studies around the Yangtze River are vital. These systems are critical for the energy and water cycle in Asian monsoon regions and are a primary cause of flood disasters in East Asia. Understanding their behavior is essential for predicting regional and global climate changes. Modern climate modeling efforts are increasingly employing large ensemble simulations to better capture the variability and potential for extreme events associated with phenomena like the Meiyu [11].

A joint field experiment by the Japan Agency for Marine-Earth Science Technology (JAMSTEC) and the Chinese Academy of Meteorological Sciences (CAMS) was conducted in 2001 and 2002 to study heavy rainfall downstream of the Yangtze River. During its intensive observational period (IOP), weather radars, a wind profiler radar, automated weather stations, and a network of soundings were deployed to analyze precipitating cloud systems. The insights gained from such field experiments are critical for refining precipitation classification algorithms and understanding hydrometeor characteristics, which remain active areas of research in atmospheric science [12, 13] surface meteorological stations [9].

Given the limited opportunities to observe frequent Meiyu frontal heavy rainfall, studies around the Yangtze River are vital. These systems are critical for the energy and water cycle in Asian monsoon regions and are a primary cause of flood disasters in East Asia. Understanding their behavior is essential for predicting regional and global climate changes.

### Instrumentation and Data Base

The primary instrument used for estimation of vertical profiles of DSD parameters is L-band wind profiler radar operated at 1290 MHz. At this frequency, the wind profiler is more sensitive to precipitation echoes than clear-air echoes that are dominant in profiler Doppler spectra of VHF frequencies (i.e., 50 and 404MHz). One vertical beam and two off-vertical beams in the orthogonal directions are currently used and the off-vertical beams are tilted 15 degrees from the zenith direction. Measured radial velocities along each beam are used to calculate wind speed and direction. Three moments of signal-to-noise ratio (SNR), Doppler velocity, and spectral width area also calculated from observed Doppler power spectra (256-FFTpoints) at each range gate height. The Doppler spectra data observed along the vertical beam were only used for vertical structure of precipitating clouds and retrievals of DSDs/rainfall parameters in this study. Time and height resolution of the data is 3 min and ~200 m, respectively. At highmode, the maximum height is ~11.0 km msl. The details of the WPR parameters are listed in Table 1.

Table 1 Operational Parameters of the 1290-Mhz Wind Profiler Radar

Parameter	Specification
Radar Wavelength	23 cm
Beam width	6°
Pulse width	1400 ns
Inter Pulse Period	71000 ns
Number of coherent integrations	40
Number of spectral averages	32

Number of FFT points	256
Height resolution	~ 200
Number of range gates	55

In this study, simultaneous observations from L-band Wind profiler radar, X-band Doppler Radar and surface meteorological data collected between 15 June to 15 July during IOP-1 and IOP-2 at Dongshan are used to understand the vertical structure of Meiyu precipitating clouds characteristics and retrieval of Raindrop Size Distribution profiles over Dongshan.

### Vertical Structure of The Meiyu Precipitating Clouds

In this section, typical observations recorded by the WPR illustrate the vertical structure and temporal evolution of precipitating cloud systems during IOP-2001 and IOP-2002. The observations will be presented to illustrate the typical structure of convective systems experienced at the experimental site, Dongshan. The shape of the Doppler spectra is characterized by the first three spectral moment information of the hydrometeors in the precipitating cloud systems. The moments yield the reflectivity of the hydrometeors, the reflectivity-weighted fall speed of the hydrometeors and the variance of the hydrometeor fall speeds within the observing volume.

The weather map remains one of the key tools for the study of atmospheric processes and the prediction of the weather. The synoptic situation during (for 23, 24 and 25 July 2001 at 00 UT) the observation period is shown in Figure 1. On 23 June 2001, a medium scale disturbance (Meiyu front) was generated near East China Sea and propagated to south of the wind profiler site. Typhoon Chebi (0102), located at South China Sea was traveling towards northward. From Fig.1(b) it can be noticed that the Meiyu front was stationary around the experimental site. The Tropical Cyclone (0102) Chebi was downgraded from Typhoon and become extra-tropical low at 24.8°N 119.4°E at Taiwan Strait, moved northward. The stationary Meiyu front moved to north of the experimental site on 25 June 2001.

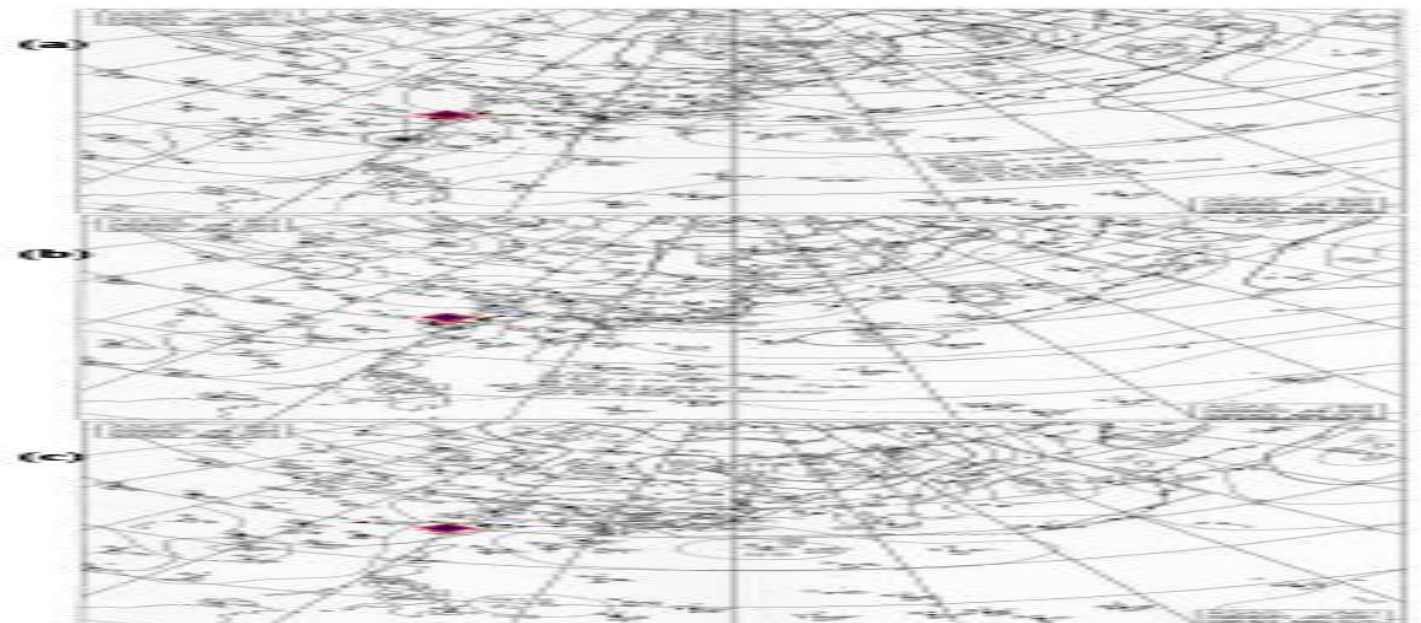


Fig.1 Surface weather chart for 22, 23 and 24 June 2001, 00 UTC. The diamond mark denotes the location of the WPR site, Dongshan.

Wind Profiler Radar (WPR) illustrate the vertical structure and temporal evolution of precipitating cloud systems during IOP-2001 and IOP-2002 (as shown in Fig.2). The shape of the Doppler spectra is characterized by the first three spectral moment information of the hydrometeors in the precipitating cloud systems. The moments yield the reflectivity of the hydrometeors, the reflectivity-weighted fall speed of the hydrometeors



and the variance of the hydrometeor fall speeds within the observing volume [14]. The primary importance of this section is to obtain vertical air motion and inferences on microphysical structure during Meiyu period. During IOP-2001 and IOP-2002, many interesting characteristics of the mesoscale convection in this region were found. On 23 June 2001, a medium scale disturbance (Meiyu front) was generated near East China Sea and propagated to south of the wind profiler site. Typhoon Chebi (0102), located at South China Sea was traveling towards northward. From GMS satellite (not shown here) images it can be noticed that the Meiyu front was stationary around the experimental site. The Tropical Cyclone (0102) Chebi was downgraded from Typhoon and become extra-tropical low at  $24.8^{\circ}\text{N}$   $119.4^{\circ}\text{E}$  at Taiwan Strait, moved northward. The stationary Meiyu front moved to north of the experimental site on 25 June 2001.

In this section, typical observations recorded by the Dongshan-Wind A time-height cross-section of reflectivity (SNR) obtained from 22-24 June 2001 during Meiyu frontal system and influence of the Typhoon Chebi (0102) is shown in Figure 2(a). Several different types of the vertical structure are evident in this figure during periods of rainfall recorded at the surface by the influence of Typhoon and Meiyu frontal system. Variations in precipitation concentration are apparent as vertical streaks in Reflectivity above 2 km. This suggests that rain mass concentration was mixed horizontally by increasing wind shear and associated turbulent eddies in the lowest 2 km. Likewise, the bright-band (layer of enhanced reflectivity) near 4.5 km reveals a time-varying intensity and small fluctuation in height. During the passage of typhoon Chebi, the heavier rain episodes occurred between 15:30 hrs and 22:30 hrs on the 23<sup>rd</sup> June illustrated a mixture of convection with stratiform rain. The Doppler vertical velocity field  $W_d$  [ $W_d = w + W_T$ , where  $w$  is vertical air motion and  $W_T$  is the particle terminal fall speed] in Fig. 2(b) reveals a largely stratiform structure, with primarily  $-1$  to  $-2$  m/s (downward) velocities characteristic of snowfall speeds above the melting region. Positive  $W_d$  within the upper levels (6-8 km) implied weak updrafts of 1-2 m/s between 0300 and 1100 LT on 24 June 2001 during the passage of Meiyu frontal precipitating cloud system. Significant updraft was not prevalent in this portion of the suggests a turbulent layer depth of about 1.5 km. The rain mass concentration becomes increasingly uniform between the melting level and the surface. mesoscale precipitating cloud system. From inspection of time vs. height sections of vertical beam measurements of mean velocity and Doppler spectrum variance, it appears that the boundary layer depth was  $\sim 2$  km through the period of high winds. The turbulent layer ( $< 2$  km) is characterized by high values of spectrum width,  $\sigma_v$  [Fig. 2(c)] and fluctuations of  $W_d$ . During the strongest wind conditions,  $\sigma_v$

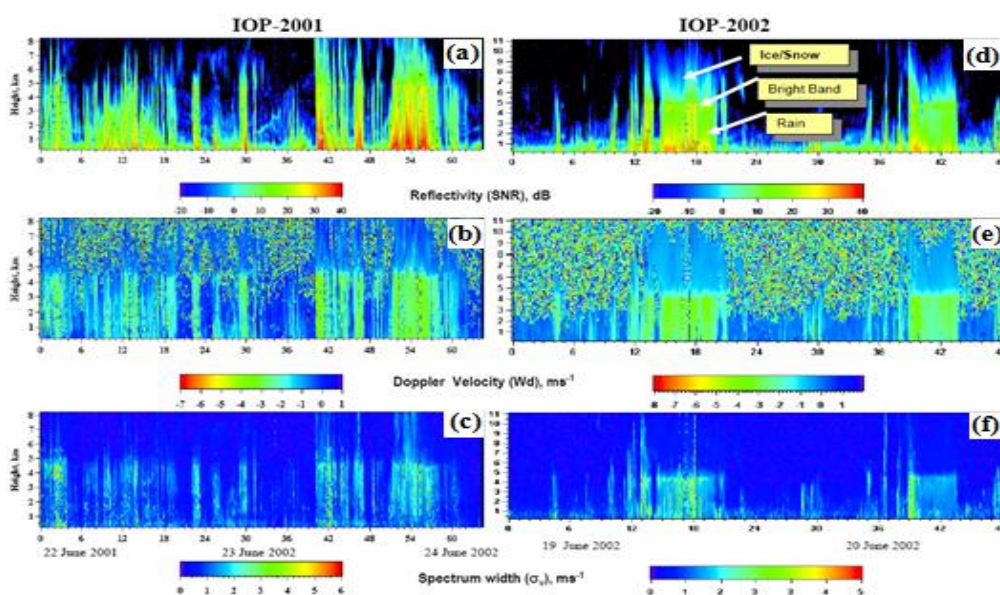


Fig.2 Vertical structure of the precipitating cloud systems observed during IOP-2001 (left three panels) and IOP-2002 (Right three panels). Time-height cross section of [top two panels (a) & (d)] Reflectivity (SNR), dB; [middle two panels (b) & (e)] Doppler velocity, m/s; and [bottom two panels (c) & (f)] Doppler spectrum width, m/s.

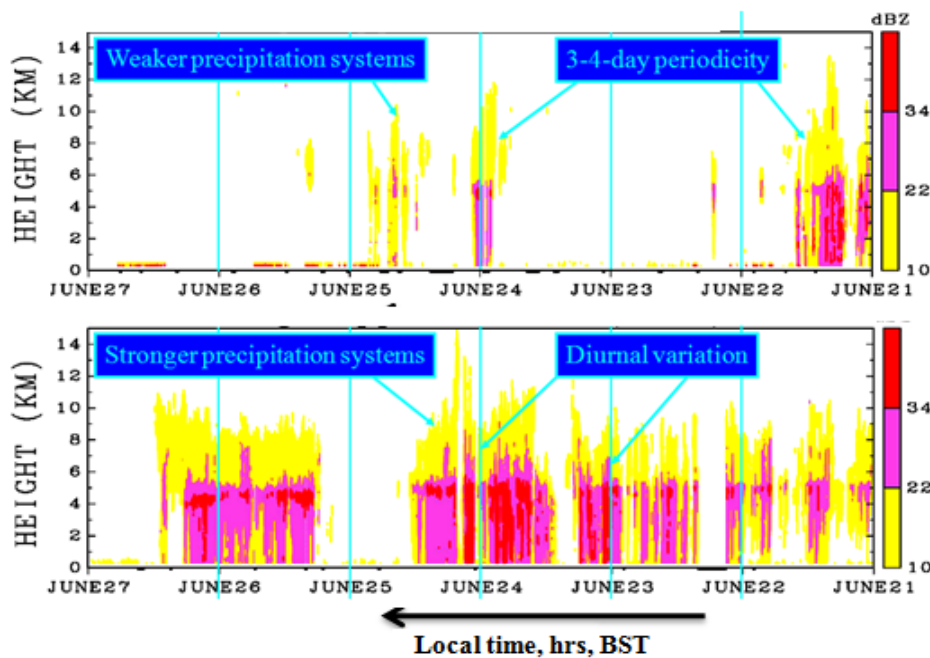


Fig.3: Time-height cross section of Radar reflectivity observed during IOP-2001 and IOP-2002 over Dongshan using X-band Doppler Radar from 21<sup>st</sup> to 27<sup>th</sup> June.

From Dongshan X-band Doppler Radar (Figure 3) observations illustrates that during IOP-2001 number days precipitation is very less compared with IOP-2002. Moreover, pronounced diurnal variation of precipitating clouds are noticed during IOP-2002.

### Formulas for Wpr-Derived Parameters

Wind profiler radars (WPRs) are valuable tools for atmospheric research, particularly in measuring precipitation and wind characteristics. Several studies focus on methodologies and algorithms to derive accurate parameters related to precipitation from WPR data (Kanofsky & Chilson, 2008)[1] (Radenz et al., 2018)[2] (Campos et al., 2007)[3] . Here's an overview of the formulas and methods used to derive precipitation parameters from wind profiler radar data:

The parameters (equivalent radar reflectivity factor, Doppler vertical velocity, and spectral width) are derived from the three moments of the Doppler power spectrum,  $S(v)$ , measured by the Wind Profiler Radar (WPR). The Doppler spectrum  $S(v)$  represents the power returned at different Doppler velocities  $v$ .

### Equivalent Radar Reflectivity Factor ( $Z_e$ )

The equivalent radar reflectivity factor ( $Z_e$ ), often expressed in dBZ (decibels relative to Z), is a measure of the radar reflectivity of a volume of atmosphere. It's proportional to the sum of the sixth power of the diameters of the hydrometeors in a unit volume.

The fundamental formula for radar reflectivity factor ( $Z$ ) for a collection of spherical raindrops is:

$$Z_e = \int N(D) * D^6 dD$$

$$dBZ = 10 * \log_{10}(Z_e) \quad (2)$$

(1)

Where:

$N(D)$ : Drop size distribution (drops per unit volume per unit size interval)

$D$ : Diameter of the raindrop (mm)

## Doppler Vertical Velocity (W)

Doppler vertical velocity ( $w$ ) represents the component of the hydrometeor's velocity along the radar beam that is directed vertically. In an ideal upward-pointing vertically-profiling radar, the measured Doppler velocity ( $V_d$ ) directly gives the vertical velocity of the hydrometeors relative to the radar. However, this is usually a combination of air motion and fall speed.

The measured Doppler velocity  $V_d$  is positive for motion away from the radar (downward for a vertically pointing radar) and negative for motion towards the radar (upward for a vertically pointing radar).

$$V_d = w_{\text{air}} + V_{\text{fall}} \quad (3)$$

where:

$V_d$  is the measured Doppler velocity (in m/s).

$w_{\text{air}}$  is the vertical air motion (updrafts/downdrafts, in m/s). By meteorological convention, positive  $w_{\text{air}}$  is upward.

$V_{\text{fall}}$  is the hydrometeor's fall speed relative to the air (terminal velocity, in m/s). This is typically negative (downward).

To isolate the *air's* vertical velocity ( $w$ ), one needs to account for the terminal fall speed of the hydrometeors ( $V_{\text{fall}}$ ). This is often done by assuming a relationship between reflectivity and fall speed (e.g., for rain) or by using multiple frequency radars.

For a vertically-pointing radar:  $w = V_d - V_{\text{fall}}$

Where  $V_{\text{fall}}$  for raindrops can be estimated using empirical relations like:  $V_{\text{fall}}(D) = cD^x$  (where  $c$  and  $x$  are constants) or more complex models, or by using the mean Doppler velocity and assuming a mean fall spe (4)

## Spectral Width ( $\sigma_v$ )

Spectral width ( $\sigma_v$ ) is a measure of the spread or dispersion of Doppler velocities within a single radar resolution volume. It quantifies the variability of velocities of the hydrometeors. A larger spectral width indicates a wider range of velocities present in the volume.

The spectral width is calculated from the second moment of the Doppler power spectrum  $S(v)$ :

$$(5) \quad \sigma_v = \sqrt{\frac{\int (v - \bar{v})^2 S(v) dv}{\int S(v) dv}}$$

where:

$\sigma_v$  is the spectral width (in m/s).

$v$  is the Doppler velocity (in m/s).

$\bar{v}$  is the mean Doppler velocity (first moment of the spectrum, which is equivalent to  $V_d$ ).

$S(v)$  is the Doppler power spectrum, representing the power contributed by targets moving at velocity  $v$ .

## Classification of Meiyuprecipitatng Clouds

The Dongshan- Wind Profiler Radar (WPR) data had a vertical resolution of 200 m and time resolution of about 90 sec. Using data derived from WPR, Reddy et al. [17] have shown that WPR can be used to classify precipitating cloud types by slightly modifying the algorithm proposed by Williams et al. [18]. In this study, WPR data obtained by the vertically pointing beam are analyzed to classify precipitating cloud types.

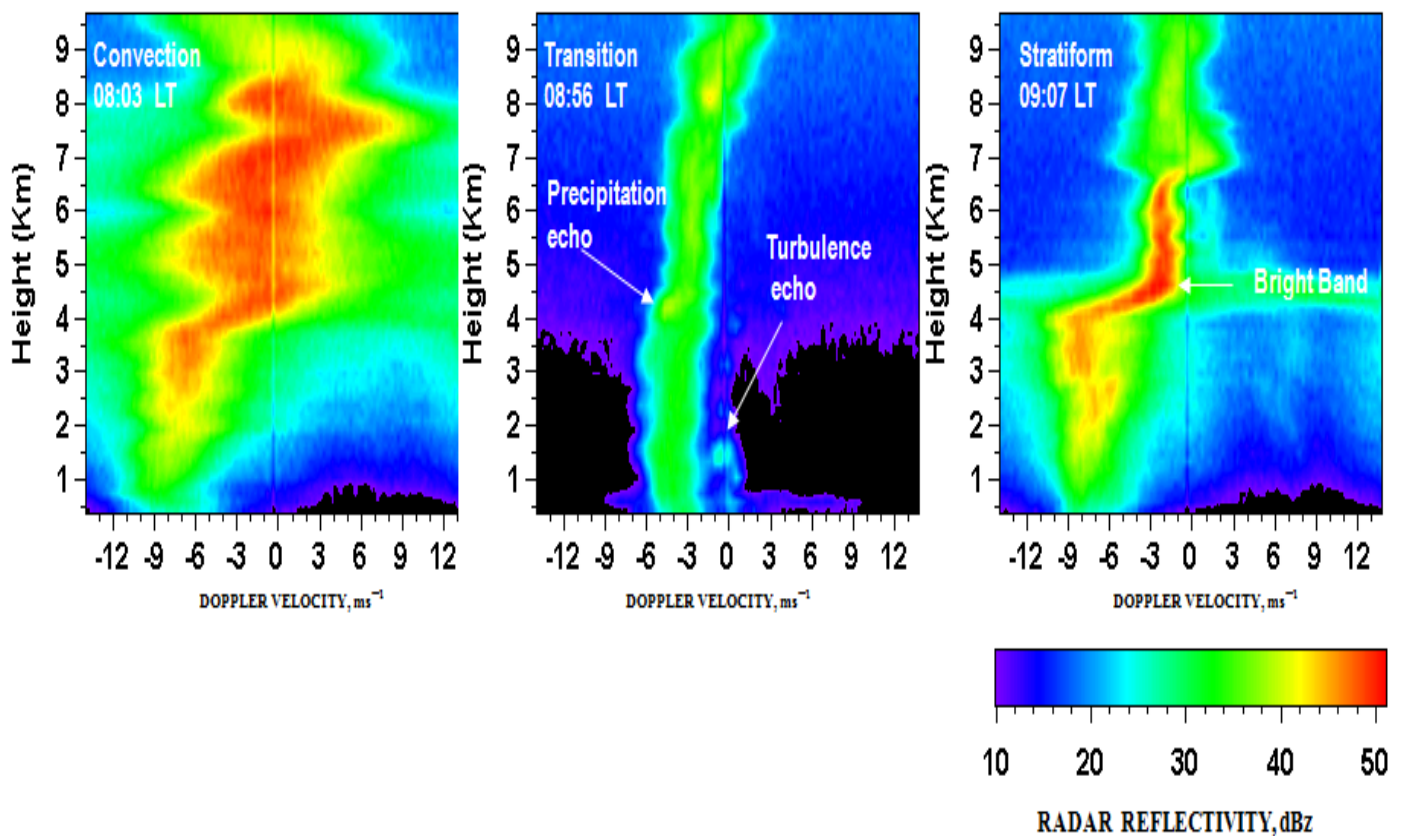


Fig 4: Doppler spectra observed during (a) convection (b) transition and (c) stratiform precipitation observed on 21 June 2001.

Typical examples of the Doppler spectra observed by the Dongshan-WPR on 21 June 2001 during convection, transition and stratiform periods of a mesoscale convective system (MCS) are shown in Fig. 4 [(a)-(c)]. The positive Doppler velocity indicates upward motion. The convective region is characterized by Doppler vertical velocities, which are greater than the typical fall speeds of ice crystals or snow [greater than approximately  $1\text{--}3\text{ ms}^{-1}$  Fig. 4(a)]. Precipitating particles grow primarily by accretion of liquid water. Ice particles in the upper levels of convective clouds often grow by rimming in the convective updrafts. Due to the relatively strong updrafts in convective regions the radar reflectivity shows well-defined vertically oriented cores of maximum reflectivity. The relatively large velocities lead to intense turbulence. The Doppler spectra in the transition period [Fig. 5.5(b)] show two echoes up to a height of  $\sim 1\text{ km}$ . The echo near the zero Dopplers shifts corresponds to that of the background air, while the echo on the negative side of the Doppler spectrum is due to the hydrometeors. The hydrometeor radar reflectivity factor and Doppler velocity are found to be smaller during the transition period compared to the convection. In contrast to the convective region, stratiform precipitation occurs when the vertical air velocity is much less than the terminal fall velocity of snow particles. With this condition, ice particles in the upper levels of clouds must fall and all the growth of the precipitating particles must occur while falling. At high levels the ice particles grow mainly by vapour deposition. When they descend to within about  $2.5\text{ km}$  of the freezing level (about  $4.5\text{ km}$ ), aggregation and rimming can occur. At upper levels the ice crystals, which have formed in a region of predominantly super-cooled water, undergo a Bergeron process. In a Bergeron process, ice crystals increase in size by diffusion of water vapour from neighbouring water droplets due to the lower saturation vapour pressure of ice. The melting layer in the stratiform region is often evident as a horizontal band of high radar reflectivity approximately  $0.5\text{ km}$  thick as shown in Fig. 4. Doppler spectra observed during (a) convection (b) transition and (c) stratiform precipitation observed on 21<sup>st</sup> June 2001.

The classification of precipitating clouds in this study is based on the algorithm adopted from Reddy et al. [17] and originated from Williams et al. [18]. As shown in Fig. 5, in the present study each sample of data is analyzed to determine which of three types of precipitating clouds, that is, stratiform, mixed/transition stratiform-convective, and convective clouds (hereinafter referred to as S, T and C, respectively), came from.



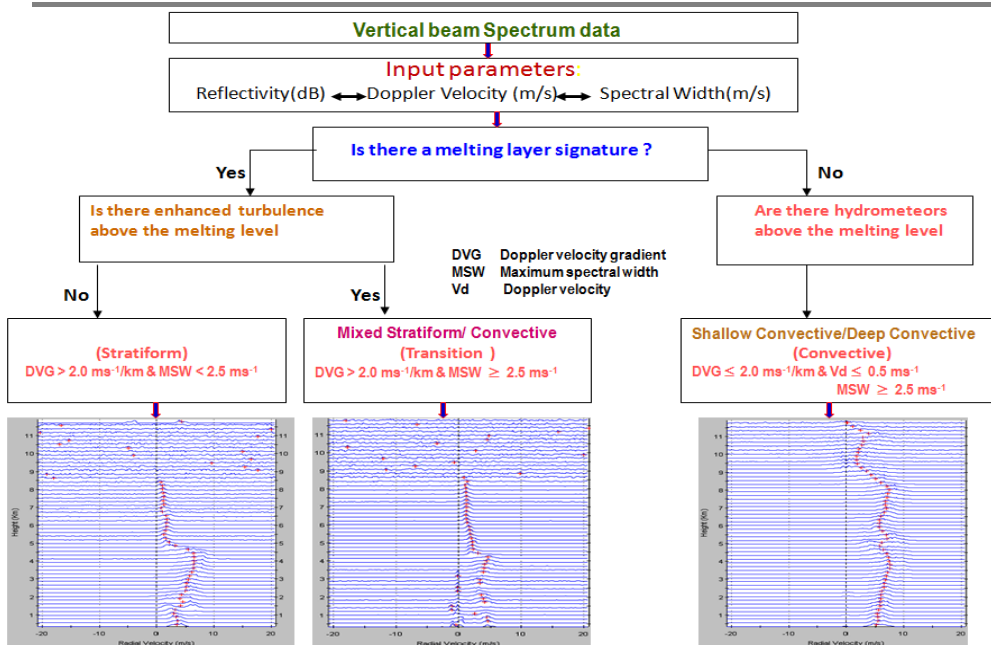


Fig.5: Classification of precipitating clouds based on the algorithm

The algorithm to classify precipitating clouds is based on a judgment of the presence of a melting layer and the presence of turbulence or hydrometeors above the melting layer. If WPR data reveal the existence of a melting layer (i.e., large received signal at 0°C isotherm level), a precipitating cloud type is classified as S or T. If WPR data do not show the existence of a melting layer, the precipitating cloud type is classified as C. Mixed type is classified if a broadening of spectral width above the melting layer, which indicates turbulent motion above the melting layer, is observed. C is classified if hydrometeors (i.e., presence of echoes) appears above the melting level. For more details of the classification method [17,18].

Figure 6 shows the time-height section of a convective system passing over Dongshan-WPR on 19<sup>th</sup> June 2002. Figure 6(a), (b) and (c) shows the equivalent radar reflectivity factor (dBZ), Doppler vertical velocity and spectral width of hydrometeors. The letters C, T and S indicate convective, transition and stratiform precipitating cloud systems, respectively.

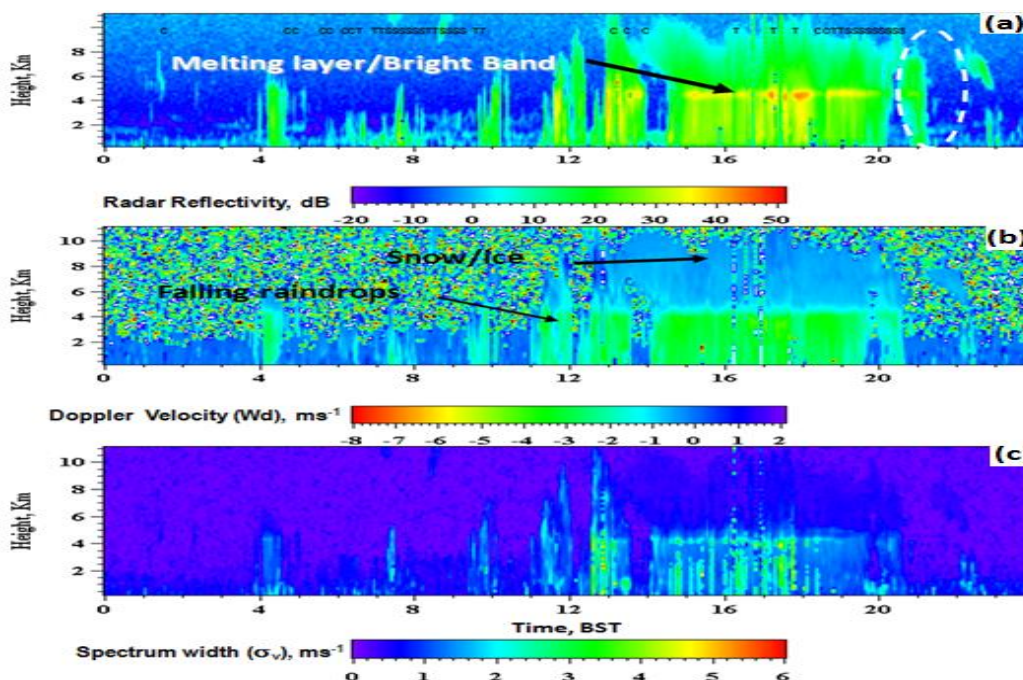


Fig.6: Time-height cross section of mesoscale Precipitating cloud system observed on 19<sup>th</sup> June 2002. (a) Radar Reflectivity, dB; (b) Doppler Velocity, m/s and Spectral Width, m/s



Figures 6 illustrate the Dongshan WPR potential for diagnosing the vertical structure of precipitating cloud systems. The reflectivity in Fig. 6(a) shows a distinct episode of convective activity, and a bright band of high reflectivity associated with a melting layer is visible. The acceleration of falling hydrometeors is evident from Fig. 6(b), showing clearly the existence of a melting layer near 4.5 km. The ability of the Dongshan-WPR to clearly resolve the melting layer when it is present also provides a means of differentiation between stratiform and convective precipitation.

To investigate the rainfall type over the observation site, classifications of precipitating clouds are performed by using WPR data. Reflectivity, Doppler velocity and spectral width derived from the vertically-pointing beam are used to determine the precipitating cloud type. For the classification of precipitating clouds, we used similar algorithm of Reddy et al. [15]. Precipitating clouds are classified into three types [stratiform, mixed convective-stratiform (transition) and convective]. In the algorithm for classification, both the existence of melting layer and the existence of enhanced turbulence above the melting level are examined [see Figure 4 of Williams et al., (16)]. If a melting layer exists and enhanced turbulence exists (does not exist) above the melting level, a precipitating cloud is classified as mixed stratiform/convective or transition (stratiform) type. If a melting layer does not exist and enhanced turbulence exists (does not exist) above the melting level, a precipitating cloud is classified into deep/shallow convective type. Figure 8 shows the time variation of precipitating cloud types during IOP-2001 and IOP-2002. During IOP-2001 precipitating clouds are dominated by mixed and stratiform type. During IOP-2002, both convective-type and stratiform –type precipitating clouds are observed over the observation site.

Microphysical or cloud-modeling studies require knowledge on the precipitating cloud type to understand the mechanism for precipitation development and to parameterize these processes in cloud-scale and mesoscale numerical models. The lower atmospheric wind profiler radars (WPRs) can provide the climatology of vertical structure of the precipitating cloud systems during Meiyu period. Figure 7 shows the observation results of the three types of precipitating cloud systems at Dongshan during (a) IOP-2001 and (b) IOP-2002. From the figure it is evident that the occurrence of stratiform clouds is different from that of convective clouds

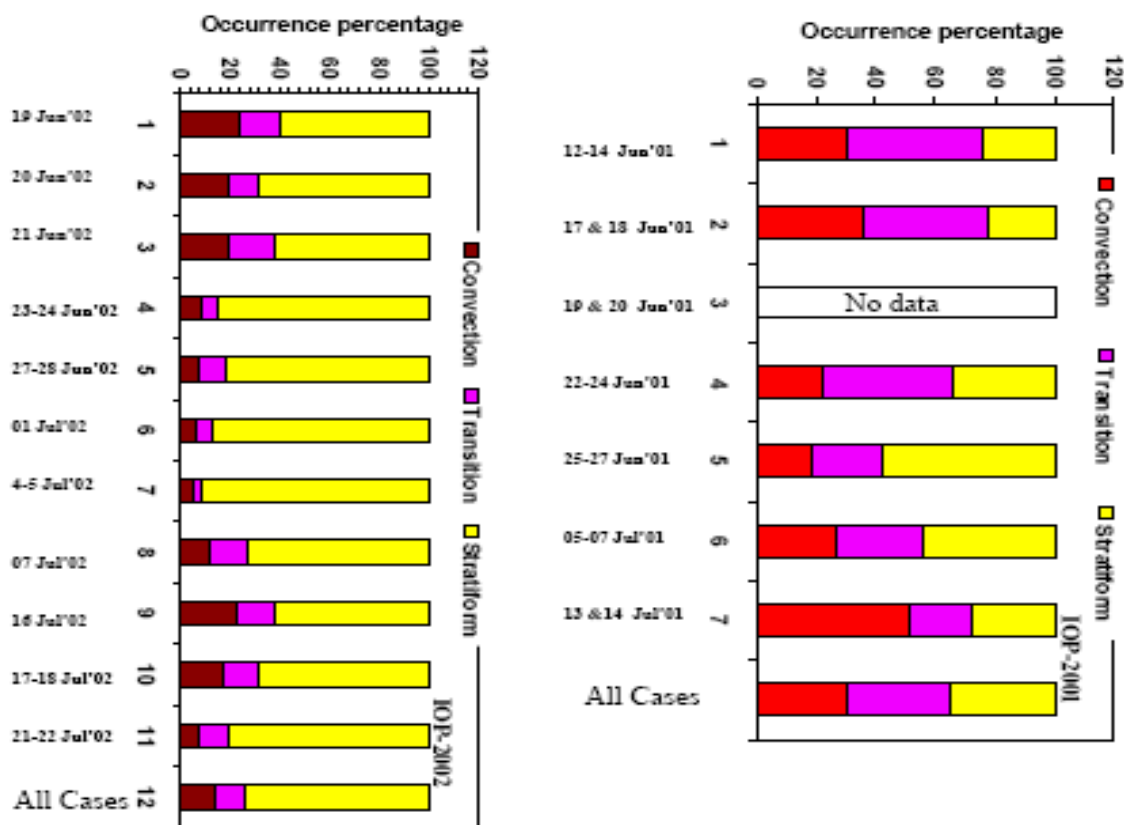


Fig.7: Occurrence percentage of three [Convective, Transition (convective/ stratiform) and Stratiform] precipitating cloud systems observed during IOP-2001 and IOP-2002 in the Meiyu period.

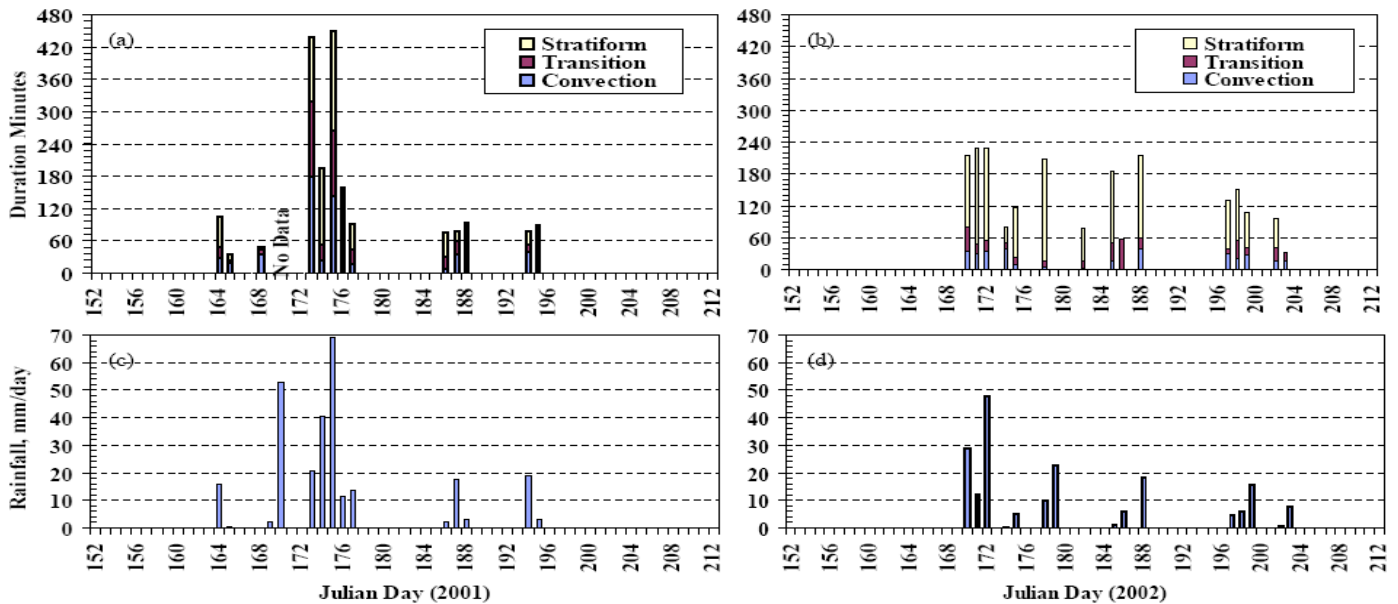


Fig.8 Time variation of precipitating cloud types classified by the Wind profiler during (a) IOP-2001 and (b) IOP-2002. Automatic Weather Station observed Daily rainfall over Dongshan during (c) IOP-2001 and (d) IOP-2002.

Convective Available Potential Energy (CAPE), Convection Inhibition (CIN), relative humidity and precipitable varied considerably around Shanghai region as shown in Figure 9 during IOP-2001 and IOP-2002. There was weak association between CAPE and environmental flow. From these figures it is evident that in the IOP-2001 and in IOP-2002 are mainly due to the difference in the distribution of water vapor and local environmental conditions. These observational results suggest that large difference in relative humidity and precipitable water.

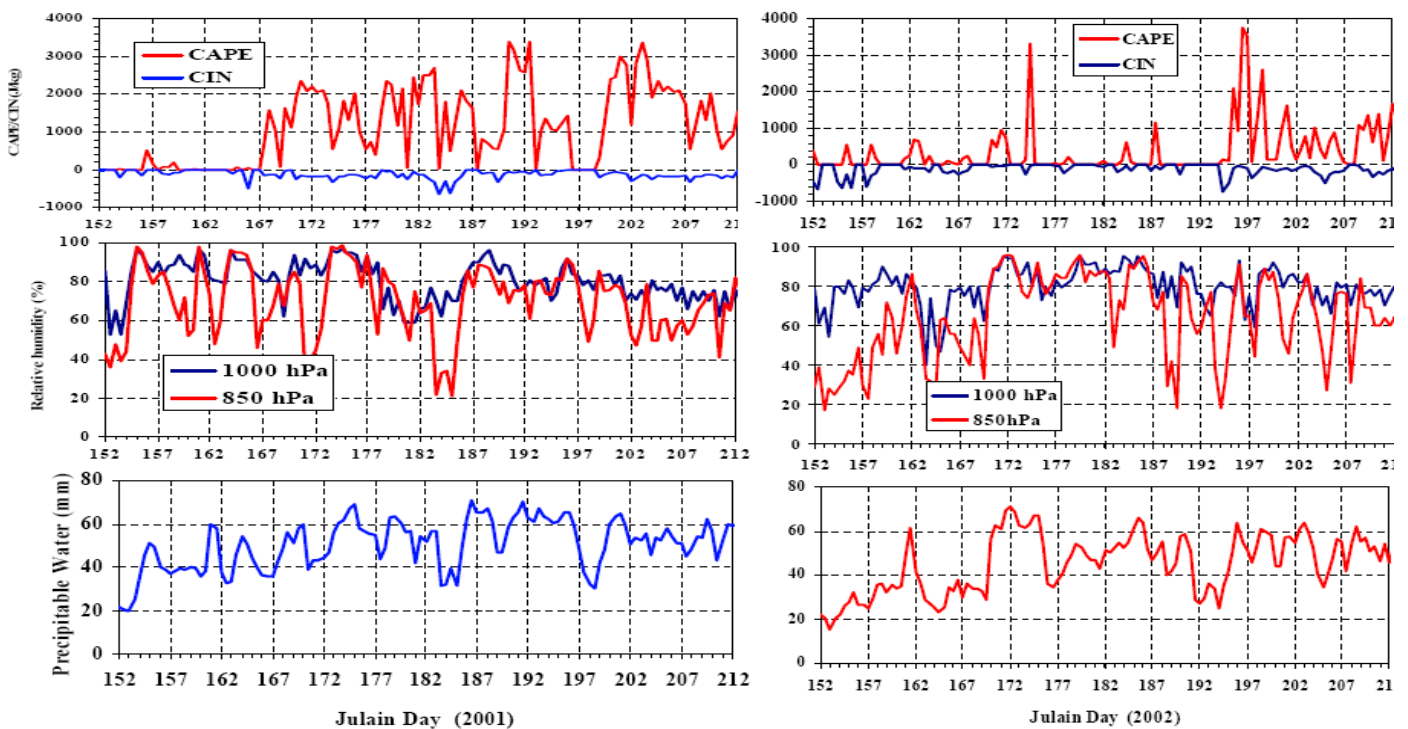


Fig.9 Characteristics of Meiyu season environmental conditions during IOP-2001 and IOP-2002. Time series of [(a) & (d)] CAPE and CIN, Relative humidity [(b) & (e)] and Precipitable water (mm) [(c) & (f)] during IOP-2001 (left panels) and IOP-2002 (right panels).

---

## SUMMARY AND DISUCSSIONS

This research paper, investigated the vertical structure and temporal evolution of Meiyu precipitating cloud systems. The primary instrument used was an L-band Wind Profiler Radar (WPR) located in Dongshan, China, with data collected during the Intensive Observation Periods (IOPs) of 2001 and 2002. The paper examined the synoptic environment during the Meiyu season, specifically highlighting the interaction between a Meiyu front and Typhoon Chebi (0102) in June 2001. Observations showed the Meiyu front remaining stationary around Dongshan while the typhoon transitioned and moved northward, influencing the frontal system's subsequent shift.

Detailed WPR observations from June 22-24, 2001, revealed diverse vertical structures in rainfall events. Reflectivity patterns showed vertical streaks, indicating horizontal mixing of rain mass by wind shear and turbulence in the lowest 2 km. A prominent "bright band" of enhanced reflectivity was consistently observed near 4.5 km, characteristic of stratiform precipitation. Doppler vertical velocity data predominantly indicated downward velocities above the melting layer, typical of stratiform structures, with occasional weak updrafts within the Meiyu frontal system. The boundary layer depth was estimated to be around 2 km, characterized by high spectral width values.

Comparisons using the Dongshan X-band Doppler Radar showed significantly less precipitation during IOP-2001 compared to IOP-2002. IOP-2002 also exhibited pronounced diurnal variations in precipitating clouds.

A crucial aspect of the study was the classification of Meiyu precipitating clouds into three types: convective, transition (mixed convective-stratiform), and stratiform. This classification was successfully achieved using a WPR-based algorithm that leveraged the presence or absence of a melting layer and the characteristics of turbulence/ hydrometeors above it. Convective regions were identified by strong updrafts, high reflectivity cores, and significant turbulence, while stratiform regions showed weaker vertical velocities, ice particle growth by vapor deposition, and a distinct bright band.

The analysis of occurrence percentages revealed distinct distributions of stratiform and convective clouds between the two IOPs. IOP-2001 was predominantly characterized by mixed and stratiform types, whereas IOP-2002 showed a more balanced presence of both convective and stratiform clouds. These variations were linked to differences in atmospheric moisture content (relative humidity and precipitable water) and local environmental conditions such as Convective Available Potential Energy (CAPE) and Convection Inhibition (CIN).

## CONCLUSIONS

The study underscored the intricate interplay between the Meiyu front and tropical cyclones (e.g., Typhoon Chebi) in shaping Meiyu rainfall characteristics. Their movement and interaction were shown to significantly influence precipitation types and intensity.

The classification algorithm, leveraging WPR data (reflectivity, Doppler velocity, and spectral width) and focusing on the presence of a melting layer and turbulence, successfully categorized Meiyu precipitation. This provides valuable insights into the dominant rainfall mechanisms during this crucial season.

**Influence of Environmental Conditions:** Significant differences observed in the dominant precipitating cloud types between IOP-2001 and IOP-2002 were directly linked to variations in atmospheric moisture content (relative humidity and precipitable water) and local environmental conditions (e.g., CAPE and CIN). This emphasizes the critical role of these factors in modulating Meiyu rainfall.

The findings highlight the immense utility of WPR data for understanding precipitation development mechanisms. This understanding is crucial for parameterizing these processes in cloud-scale and mesoscale numerical models, which will ultimately contribute to improved Meiyu rainfall predictions and enhanced flood disaster mitigation efforts in East Asia.

In essence, this study provides a valuable contribution to the climatology of vertical structures of precipitating cloud systems during the Meiyu period, serving as a vital resource for both regional climate change studies and disaster preparedness in East Asia.

## ACKNOWLEDGEMENTS

The authors wish to express their sincere gratitude to the Institute of Observational Research for Global Change (IORGC), Japan Agency for Marine-Earth Science and Technology (JAMSTEC), Japan, for collecting and providing the original data used in this research. We are also deeply thankful to the researchers from JAMSTEC and the Chinese Meteorological Administration (CAMS), China, for their invaluable involvement and contributions.

## REFERENCES:

1. Wang, X., Dong, X., Deng, Y., Cui, C., Wan, R., & Cui, W. (2019). Contrasting Pre-Mei-Yu and Mei-Yu Extreme Precipitation in the Yangtze River Valley: Influencing Systems and Precipitation Mechanisms. *Journal of Hydrometeorology*, 20(9), 1961–1980. <https://doi.org/10.1175/jhm-d-18-0240.1>
2. [Li, H., Hu, Y., Zhou, Z., Peng, J., & Xu, X. (2018). Characteristic Features of the Evolution of a Meiyu Frontal Rainstorm with Doppler Radar Data Assimilation. *Advances in Meteorology*, 2018, 1–17. <https://doi.org/10.1155/2018/9802360>
3. Lai, H.-C. (2011). Wind Profiler Observation on Vertical Structure of a Mei-yu Front Cloud Bands. *Journal of the Meteorological Society of Japan*. Ser. II, 89A, 307–316. <https://doi.org/10.2151/jmsj.2011-a21>
4. Liu, C., & Ding, Y. (2023). Performance of Seven Land Surface Schemes in the WRFv4.3 Model for Simulating Precipitation in the Record-Breaking Meiyu Season Over the Yangtze–Huaihe River Valley in China. *Earth and Space Science*, 10(2), e2022EA002446. <https://doi.org/10.1029/2022EA002446>
5. Chen, G. T. J., Chen, Y. L., & Chen, C. H. (1998). The influence of terrain on heavy precipitation during TAMEX. *Monthly Weather Review*, 126(11), 2908–2921.
6. Ding, Y. (1994). *Monsoon Meteorology*. Springer.
7. Lau, K.-M., & Tao, W. K. (2000). South China Sea Monsoon Experiment (SCSMEX): A field campaign to understand the Asian monsoon. *Bulletin of the American Meteorological Society*, 81(5), 993–1008.
8. Ninomiya, K. (2000). The Meiyu-Baiu front and its associated precipitation systems: A review. *Journal of the Meteorological Society of Japan*, 78(3), 349–374.
9. Shinoda, T., & Uyeda, H. (2002). Hydrological cycle in the Huaihe River Basin, China: The Huaihe River Basin Experiment (HUBEX). *Journal of the Meteorological Society of Japan*, 80(4), 719–743.
10. Li, Z., Sun, L., Han, X., & Wu, C. (2022). Radar Characteristics and Causal Analysis of Two Consecutive Tornado Events Associated with Heavy Precipitation during the Mei-Yu Season. *Remote Sensing*, 15(23), 5470. <https://doi.org/10.3390/rs15235470>
11. Lin, P., Yang, L., Zhao, B., Liu, H., Wang, P., Bai, W., ... & Ding, Y. (2025). Large ensemble simulations of climate models for climate change research: A review. *Advances in Atmospheric Sciences*, 42(5), 825–841. <https://doi.org/10.1007/s00376-024-4012-2>
12. Ren, Y., Liu, P., & Yang, K. (2024). Righting wrongs of precipitation-type classification over Tibetan Plateau with new algorithm applied to satellite radar data, *Advances in Atmospheric Sciences* 41(12):1–19. <https://DOI:10.1007/s00376-024-3384-7>
13. Pan, H., Liu, L., Wu, J., Zhang, C., & Zhao, C. (2024). Hydrometeor Classification of Winter Precipitation in Northern China Based on Multi-Platform Radar Observation System. *Remote Sensing*, 16(20), 3859. <https://doi.org/10.3390/rs16203859>
14. Gage, K. S., Balsley, B. B., Ecklund, W. L., Carter, D. A., McAfee, J. R., & Riddle, A. C. (2002). Doppler spectral characteristics of a mesoscale convective system observed with a 915 MHz wind profiler. *Journal of Applied Meteorology*, 41(4), 431–447.



15. Kanofsky, L., & Chilson, P. (2008). An Analysis of Errors in Drop Size Distribution Retrievals and Rain Bulk Parameters with a UHF Wind Profiling Radar and a Two-Dimensional Video Disdrometer. *Journal of Atmospheric and Oceanic Technology*, 25(12), 2282–2292. <https://doi.org/10.1175/2008jtecha1061.1>
16. Radenz, M., Bühl, J., Lehmann, V., Görsdorf, U., & Leinweber, R. (2018). Combining cloud radar and radar wind profiler for a value added estimate of vertical air motion and particle terminal velocity within clouds. *Atmospheric Measurement Techniques*, 11(10), 5925–5940. <https://doi.org/10.5194/amt-11-5925-2018>
17. Reddy, K. K., Das, S. K., Rao, P. B., Reddy, R. V. B., & Rao, D. N. (2005). Characterization of precipitating clouds using a lower atmospheric wind profiler at Gadanki (13.5°N, 79.2°E), a tropical station. *Journal of Geophysical Research: Atmospheres*, 110(D13). <https://doi.org/10.1029/2004JD005727>
18. Williams, C. R., Ecklund, W. L., & Gage, K. S. (1995). Classification of precipitating clouds in the tropics using 915-MHz wind profilers. *Journal of Atmospheric and Oceanic Technology*, 12(5), 996–1012.